Theory of magnetic superconductors

Helvetica Physica Acta,
Vol. 56 (1983) 189-206

0018-0238/83/010189-18$1.50+0.20/0

Theory of Magnetic Superconductors

M. Tachiki
The Research Institute for Iron, Steel and Other Metals
Tohoku University, Sendai 980, Japan

Abstract. An epoch-making discovery of new ternary compounds which are simultaneously superconductors and magnetic materials was made in 1977. Since then, many materials of this type have been found and are called "magnetic superconductors". These materials have unusual properties owing to the interplay between superconductivity and magnetism. The explanation of these properties and the predictions of new phenomena are presented.

1. Introduction

Are there materials in which superconducting order and magnetic order coexist, and if these materials exist, do some unique properties appear owing to the interplay between these two orders ? This question was posed many years ago [1]. The discovery of the rare earth ternary compounds (RE)Mo_6S_8 [2] and (RE)Rh_4B_4 [3] provided a key for answering this old problem. These compounds show superconductivity, although the rare earth magnetic ions are regularly situated at the lattice sites [4,5]. In these compounds, superconducting and magnetic orders very often occur at the same time. Experiments show that these compounds possess unusual electromagnetic properties [6]. Nowadays, these materials are called magnetic superconductors. Recently many compounds joined the magnetic superconductors. These are the examples: (RE)M_4B_4 with M = Ru [7], Ir [8], and Os [9], (RE)Rh_xSn_y [10], (RE)$_2Fe_3Si_5$ [11], (RE)$_5Co_4Si_{10}$ [12], and $CeCu_2Si_2$ [13]. In these compounds, the magnetic moments are carried by the 4f electrons of rare earth ions localized at the lattice sites and superconductivity is mainly carried by the 3d, 4d, and 5d electrons of transition metal ions.

Recently, there appears the new type of magnetic superconductors in which the magnetic order arises from itinerant electrons. The binary intermetallic compound Y_9Co_7 is a weak itinerant electron ferromagnet with the Curie temperature of 4K ∿ 6K [14]. This compound shows superconductivity below 2K ∿ 3K. The organic compound $TMTSF_2X$ with X = ClO_4 [15] is a superconductor at ambient pressure and those with X = PF_6 [16], AsF_6 [16], and TaF_6 [17] are superconductors under pressure. In the organic compounds the antiferromagnetic order appears above the superconducting transition temperature.

Owing to the interaction between the magnetic moments and the superconducting electrons, the magnetic superconductors are expected to show various kinds of unusual properties. In this paper the following topics are chosen: A long period order of magnetic moments in the superconducting state of ferromagnetic superconductors, flux quantization and anomalous magnetization curves in the mixed state, surfaces and films of ferromagnetic superconductors, and the Josephson effect in ferromagnetic superconductors. Before discussing these topics, we should mention the nature of the interaction between the magnetic moments and the superconducting electrons.

2. Interaction between the magnetic moments and the superconducting electrons

In the magnetic superconductors of the rare earth compounds, two kinds of interactions are important. One is the exchange type interaction between the magnetic ions and the conduction electrons, the so-called d-f interaction. The other is the electromagnetic interaction between the persistent current and the magnetic moments.

d-f interaction

Since this interaction forces both the spins in the singlet Cooper pair to align parallel or antiparallel to the spin of the rare earth ion, the interaction causes the breaking effect of the Cooper pair. According to this effect, the spin fluctuations and the magnetization of the rare earth ions work to decrease the superconducting transition temperature and the critical fields [18∿24]. In antiferromagnets, the periodic exchange potential produces a new energy gap in the energy band and decreases the number of electrons responsible for superconductivity. This potential also affects the wave function of superconducting electrons and weakens the BCS interaction. These effects are all accountable for the anomalous behavior of the temperature dependence of the upper critical field in antiferromagnetic superconductors.

Electromagnetic interaction

The electromagnetic interaction between the persistent current and the magnetic moments causes various kinds of phenomena, especially in ferromagnetic superconductors.

Screening effect

We write the molecular field acting on the magnetic moment at the position $\vec{x}$ in the normal state as $\int\gamma(\vec{x}-\vec{y})\vec{m}(\vec{y})d^3y$, where $\gamma(\vec{x}-\vec{y})$ is the exchange interaction constant between the magnetic moments at the positions $\vec{x}$ and $\vec{y}$ in the normal state. We use the continuum model. In the superconducting state, we should add the magnetic field induced by the persistent current $\vec{h}(\vec{x})$ to the molecular field mentioned above. Thus, the molecular field in the superconducting state is written as

$$\vec{h}_m(\vec{x}) = \int\gamma(\vec{x}-\vec{y})\vec{m}(\vec{y})d^3y + \vec{h}(\vec{x}) \ . \tag{1}$$

Since the magnetic field $\vec{h}(\vec{x})$ results from the persistent current induced by the magnetic moments, $\vec{h}(\vec{x})$ is also a linear function of $\vec{m}(\vec{x})$. Therefore, the molecular field (1) can be written in the form $\vec{h}_m(\vec{x}) = \int\tilde{\gamma}(\vec{x}-\vec{y})\vec{m}(\vec{y})d^3y$. Since $\vec{h}_m(\vec{x})$ has the lattice periodicity, $\vec{h}_m(\vec{x})$ is expanded in the Fourier series as

$$\vec{h}_m(\vec{x}) = \sum_{\vec{q}}\tilde{\gamma}(\vec{q})\vec{m}(\vec{q})\exp(i\vec{q}\cdot\vec{x}) \ . \tag{2}$$

The quantities $\tilde{\gamma}(\vec{q})$ and $\vec{m}(\vec{q})$ are respectively the Fourier transforms of $\tilde{\gamma}(\vec{x})$ and $\vec{m}(\vec{x})$. The effective interaction constant $\tilde{\gamma}(\vec{q})$ includes the screening effect due to the persistent current and the electromagnetic interaction between the magnetic moments. Since the effect and the interaction have only the transverse

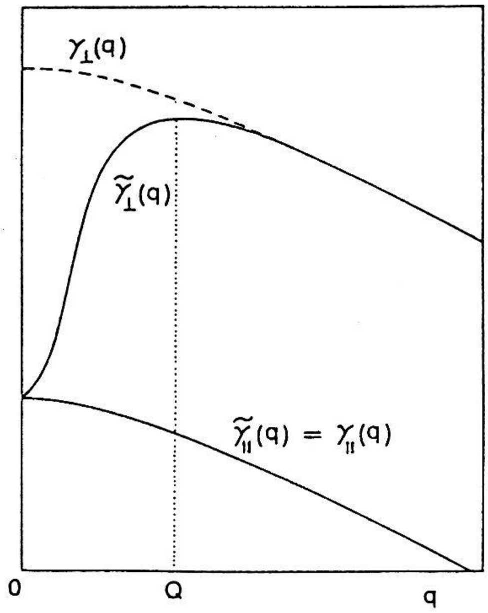

Figure 1
q-dependence of the exchange interaction constants.

components, $\tilde{\gamma}(\vec{q})$ is very anisotropic with respect to the angle between $\vec{q}$ and $\vec{m}(\vec{q})$. We write $\tilde{\gamma}(\vec{q})$ for $\vec{q}\perp\vec{m}(\vec{q})$ and $\vec{q}\parallel\vec{m}(\vec{q})$ as $\tilde{\gamma}\perp(\vec{q})$ and $\tilde{\gamma}\parallel(\vec{q})$, respectively. The wave number dependence of these quantities is shown in Fig. 1. In this figure, the exchange interaction constant in the normal state $\gamma(\vec{q})$ is also shown. The exchange constant has a maximum at $q = 0$, since the system is assumed to be ferromagnetic in the normal state. When the wave number q is smaller than $2\pi/\lambda_L$, λ_L being the London penetration depth, the interaction is strongly screened and $\tilde{\gamma}\perp(q)$ has a maximum at a finite wave number Q. Therefore, the magnetic structure stable in the superconducting state is a periodic structure [29∿32]. Since $\tilde{\gamma}\perp(Q)$ is larger than $\tilde{\gamma}\parallel(q)$ for all q as seen in Fig. 1, the magnetic moments should be perpendicular to $\vec{Q}$.

Sinusoidal magnetic order in $HoMo_6S_8$ and $ErRh_4B_4$

In a narrow temperature range above the lower transition temperature T_{c2} in $HoMo_6S_8$ and $ErRh_4B_4$, the sinusoidal order of the rare earth magnetic moments which may correspond to the magnetic structure predicted above was observed. The wavelength of the sinusoidal order is 200 Å for $HoMo_6S_8$ [33,34] and 100 Å for $ErRh_4B_4$ [35,36]. According to the experiments using the single crystals of $ErRh_4B_4$, the direction of the wave vector $\vec{Q}$ is inclined at about 45° from the c axis of the tetragonal crystal, and the magnetic moments of Er are perpendicular to $\vec{Q}$ in the c plane [36]. The fact that the magnetic moments are perpendicular to $\vec{Q}$ in the c plane is consistent with the prediction mentioned above. Just from the magnetocrystalline anisotropy, the magnetic moments can be in any direction in the c plane.

In the ferromagnetic normal state of $HoMo_6S_8$ and $ErRh_4B_4$ below T_{c2}, the samples may be divided into many magnetic domains, which are separated by domain walls. Since the magnetic structure inside the domain walls is similar to the spiral magnetic structure, the walls are possible to be superconductive under some condition [37].

The magnetic scattering of neutrons in the rare earth compounds is caused by the magnetic interaction between the magnetic moments of neutrons and the rare earth ions. The magnetic interaction is screened by the persistent current, and, therefore, the forward scattering is almost perfectly screened in the superconducting state [38].

3. Flux quantization and magnetization curve in the mixed state

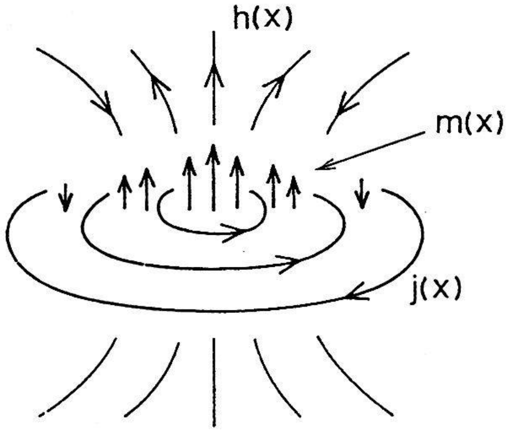

Figure 2
Magnetic field, magnetization, and current in the vortex.

Let us consider one vortex in the sample of the Meissner state. As shown in Fig. 2, the vortex current induces the magnetic field $h(\vec{x})$ and the magnetic field produces the magnetization of the rare earth ions $m(\vec{x})$ in the vortex. If we define the

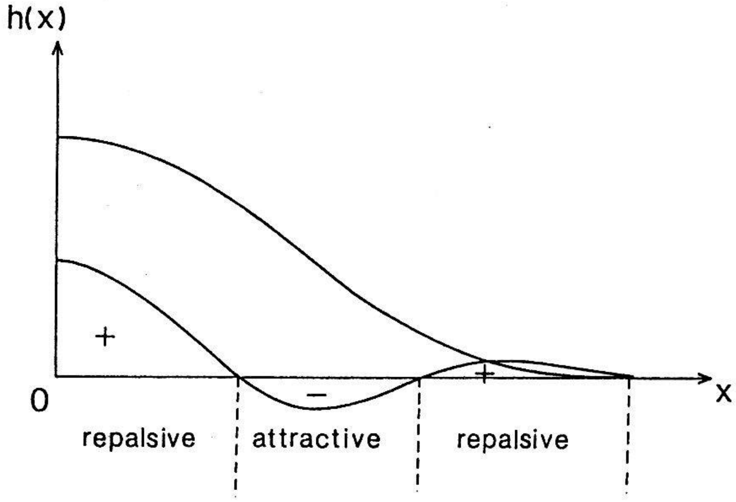

Figure 3
Spatial dependence of the magnetic field in the vortex.

magnetic induction $b(\vec{x})$ as $b(\vec{x}) = h(\vec{x}) + 4\pi m(\vec{x})$, the condition of the flux quantization is given by

$$\int b(\vec{x})d^2x = \int h(\vec{x})d^2x + 4\pi\int m(\vec{x})d^2x = \phi_0 = hc/2e\ , \qquad (3)$$

where ϕ_0 is the unit flux. The interaction energy between the two vortices $\vec{x}$ apart is shown to be proportional to $h(\vec{x})$. When $m(\vec{x})$ is negligibly small at temperatures far above the magnetic phase transition temperature T_m, $h(\vec{x})$ has a positive value as shown in Fig. 3. The zero point in this figure corresponds to the center of vortex. When $h(\vec{x})$ is positive, the repulsive interaction acts between the vortices and the triangular lattice of the vortices are constructed in the mixed state. When temperature decreases near T_m, and $m(\vec{x})$ increases, $\int h(\vec{x})d^2x$ should decrease by the restriction of the flux quantization (3). This decrease of the integral causes the decrease of $h(\vec{x})$ itself. In the case that the wave number dependence of the staggered susceptibility of the rare earth magnetic moments is strong, $h(\vec{x})$ oscillates and some part of the tail becomes negative as shown by the dashed curve in Fig. 3 [39,40]. The negative sign of $h(\vec{x})$ indicates the attractive interaction acting between the vortices. When an external magnetic field is applied near T_m, the attractive interaction causes a simultaneous entrance of many vortices at the lower critical field H_{c1}, and thus the magnetization jumps at H_{c1} [39,41].

When the external magnetic field further increases, the magnetization of the rare earth ions increases more. If the d-f exchange interaction exists, the magnetization polarizes the spins of conduction electrons through the interaction. The breaking effect of the Cooper pairs due to the spin polarization becomes stronger near the upper critical field H_{c2}. When the strength of the d-f interaction exceeds a critical value, the superconducting state abruptly changes to the normal state and the magnetization jump occurs at H_{c2} [42,43].

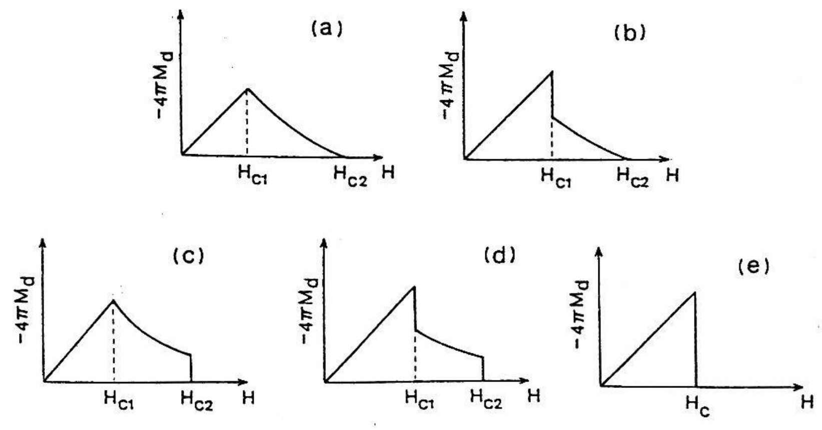

Figure 4
Various types of the diamagnetic magnetization in ferromagnetic superconductors.

The magnetic superconductors are originally the type II superconductors. However, according to the effects mentioned above, we expect many kinds of the magnetization curves occuring in the magnetic superconductors. These are schematically shown in Fig. 4. The magnetization curve in Fig. 4(a) is of usual type II superconductors. In the magnetic superconductors, the following types of magnetization curve are expected depending on material constants. The magnetization curve in Fig. 4(b) has a jump at H_{c1}, that in Fig. 4(c) has a jump at H_{c2}, and that in Fig. 4(d) has jumps both at H_{c1} and H_{c2}. Near the magnetic transition temperature, the magnitudes of the magnetization jumps at H_{c1} and H_{c2} much increases and finally the magnetization curve becomes of the type I superconductor as shown in Fig. 4(e) [43].

An example of the calculated magnetization curve is

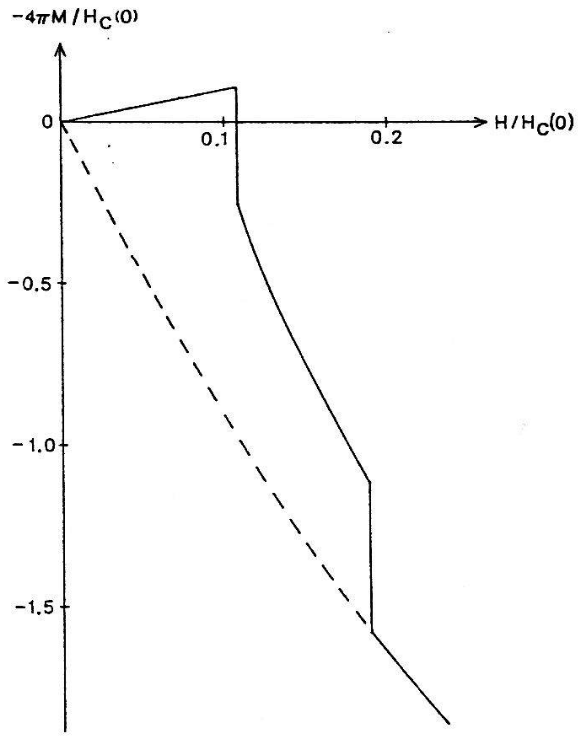

Figure 5
An example of the calculated magnetization curve.

shown in Fig. 5. This curve corresponds to that in Fig. 4(d), but the curve in the mixed state is shifted to the positive owing to the contribution of the rare earth magnetization.

Crabtree et al. [44] made the magnetization measurements using the single crystals of $ErRh_4B_4$, and obtained the magnetization curves corresponding to that in Fig. 4(c) when they applied external magnetic fields along the easy direction of magnetization.

4. Self-induced vortices and phase diagram

If we assume a uniform spontaneous magnetization of the rare earth magnetic moments M, $4\pi M$ acts on the electron motion as an external magnetic field. Therefore, if $4\pi M$ fulfills the condition

$$H_{c1}^{0} < 4\pi M < H_{c2}^{0} , \tag{4}$$

the vortices are possibly stabilized without applying an external magnetic field. In (4) H_{c1}^{0} and H_{c2}^{0} are respectively the lower

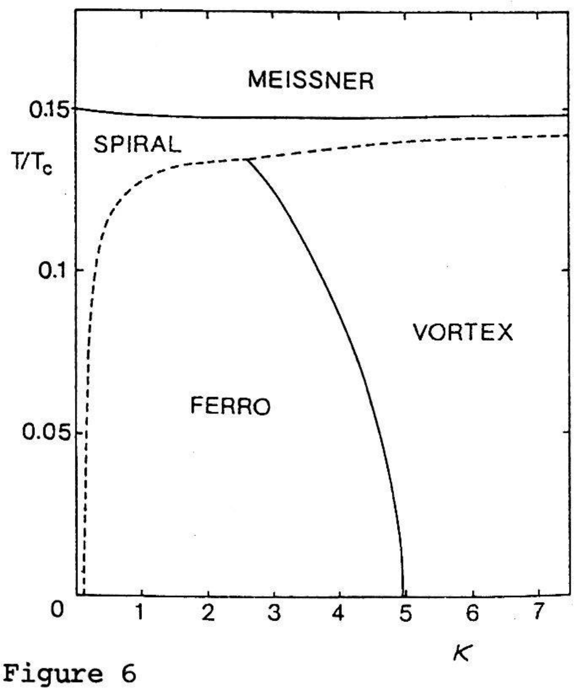

Figure 6
Phase diagram.

and upper critical fields when the magnetization vanishes. In this vortex state, the magnetization M should be stabilized by the magnetic field induced by the vortex current in a self-consistent way. Accordingly, this type of the vortices is called the self-induced vortices. The vortex state is one type of the coexistence of ferromagnetism and superconductivity [41,45,46].

Which state is stabilized in a ferromagnetic superconductor is due to its material constants. Figure 6 shows the phase diagram in the plane of the Landau parameter κ and the reduced temperature normalized by the superconducting temperature T_c [47]. As the material constants, the approximate values for $ErRh_4B_4$ were taken. The solid curves indicate the second order phase transition boundaries and the dashed curve indicates the first order phase transition boundary. When the magnetocrystalline anisotropy is strong, the spiral ordered state is replaced by the sinusoidal ordered state.

5. Surfaces and films of ferromagnetic superconductors

Let us consider the sample of ferromagnetic superconductor which has a surface at $x = 0$ and extends over the space of $x \geq 0$. The molecular field acting on the rare earth magnetic moments is expressed by the sum of the molecular field in the normal state $\vec{h}_m^{\,0}(\vec{x})$ and the screening field due to the persistent current $\vec{h}(\vec{x})$ as

$$\vec{h}_m(\vec{x}) = \vec{h}_m^{\,0}(\vec{x}) + \vec{h}(\vec{x}) \ . \tag{5}$$

When $\vec{h}(\vec{x})$ is parallel to the surface, $\vec{h}(\vec{x})$ should be continuously connected with the magnetic field in vacuum at the surface. When no external magnetic field is applied, $\vec{h}(\vec{x})$ vanishes at the surface. For this reason, the screening effect is weakened up to the depth of λ_L from the surface. Therefore, when temperature is decreased, the surface magnetization appears prior to the bulk magnetization [48∿50].

The films of ferromagnetic superconductors have the surfaces at the both sides. When the film thickness is of the order of λ_L, the surface magnetizations appearing near the both surfaces interfer inside the film. As a result, various kinds of the magnetic order occur depending on the film thickness. When the thickness is shorter than λ_L, the screening effect due to the persistent current becomes incomplete anywhere in the film, and the ferromagnetic order which is suppressed in the bulk appears in the film and coexists with superconductivity [52,53]. On the other hand, when the film thickness exceeds λ_L, the oscillatory magnetization appears owing to the screening effect inside the film.

Figure 7 shows the magnetic phase diagram in the plane of the film thickness a/λ_L and the temperature T/T_m, T_m being the ferromagnetic transition temperature of the bulk sample [53]. We assumed the uniaxial magnetic anisotropy parallel to the surface. The solid curve indicates the magnetic phase transition temperature. Below the phase transition temperature, the sinusoidal-like magnetic structure appears as shown in Fig. 7. The number of nodes in the sinusoidal-like pattern increases with the film thickness. In the temperature region below the dashed curve the normal ferromagnetic state is stable.

As seen in Fig. 7 the regions of two different natures

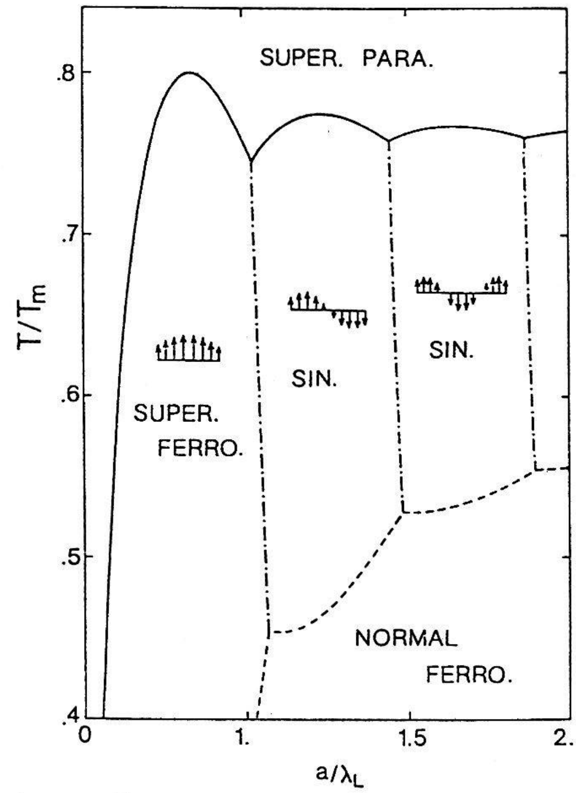

Figure 7
Phase diagram in the plane of temperature and thickness of film.

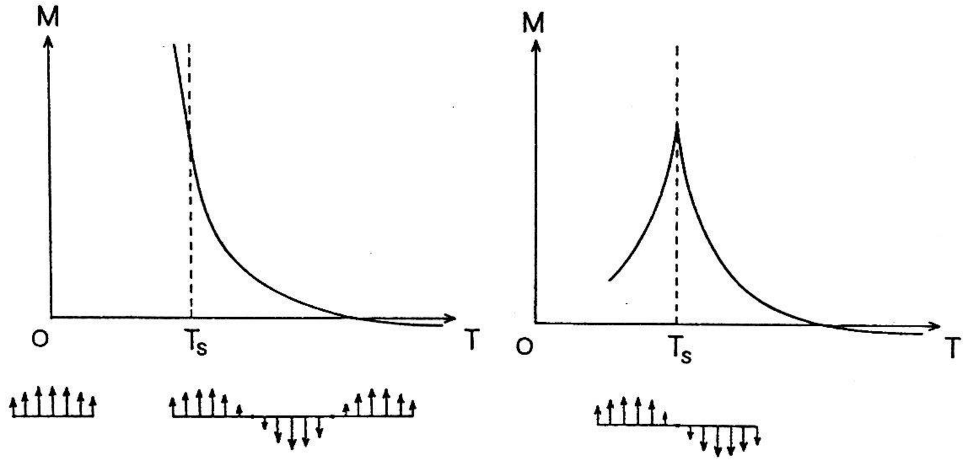

Figure 8
Magnetization of films for weak fields.

of sinusoidal orders alternately appear when the film thickness is increased. One is the ferro- or ferrimagnetic region in which the net spontaneous magnetization exists in the film. The other is the antiferromagnetic region in which the magnetic moments are cancelled inside the film. When we measure the magnetization by applying a very weak magnetic field, we expect a quite different temperature dependence of the magnetization in these two regions, as shown in Fig. 8. In the ferro- and ferrimagnetic regions the magnetization monotonically increases with decreasing temperature, but in the antiferromagnetic region the magnetization has a maximum at the phase transition temperature [54].

6. Josephson effect

Let us consider a tunnel junction made of ferromagnetic superconductors. If we write the phase difference of the superconducting order parameters of the superconductors at the left and right sides of the junction $\Delta\phi$, the Josephson tunneling current is expressed as [55]

$$J = J_c \sin\Delta\phi \quad , \tag{6}$$

where J_c is a constant which is determined by the nature of the junction. Since a very thin insulator film is inserted at the junction and the junction part is in the weak superconducting state, a faint magnetic field can penetrate the junction and affect the phase difference of the order parameters. Therefore, the Josephson current is very sensitive to the magnetic field applied at the junction. For the same reason the magnetic moments near the junction strongly influences the phase difference. Therefore, the Josephson effect in the ferromagnetic superconductors is excepted to be very unusual one [56].

If we write the coordinates along the junction as x, the differential equation for the phase difference is given by

$$\frac{d^2}{dx^2}\,\Delta\phi(x) = \frac{1}{\lambda_J{}^2(t)}\,\sin\Delta\phi(x) \tag{7}$$

with

$$\lambda_J(T) = \sqrt{\alpha(T)}\;\lambda_J \;, \tag{8}$$

$$\lambda_J = \phi_0 c/16\pi^2 J_c \lambda_L \;, \tag{9}$$

where $\lambda_J(T)$ and λ_J are the Josephson penetration depths for the

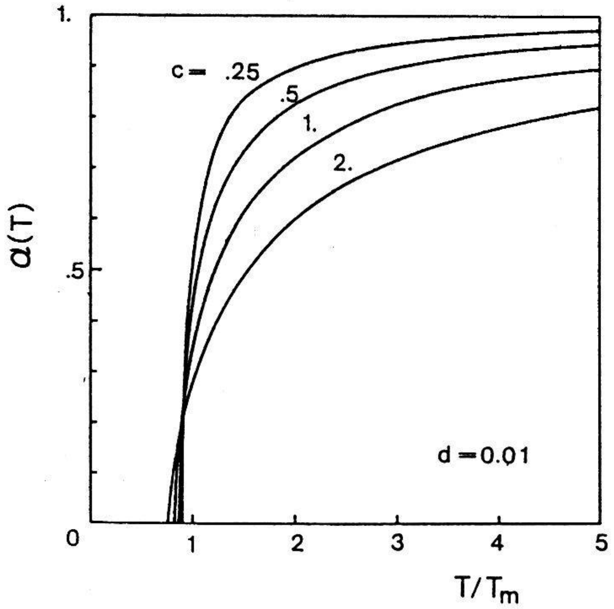

Figure 9
Temperature dependence of $\alpha(T)$.

junctions of the magnetic superconductor and nonmagnetic superconductor, respectively. The Josephson penetration depth $\lambda_J(T)$ is given by scaling λ_J by the factor $\sqrt{\alpha(T)}$. The effect of the magnetic moments is included in $\alpha(T)$. The calculated temperature dependence of $\alpha(T)$ is shown in Fig. 9. As seen in the figure, $\alpha(T)$ decreases with decreasing temperature and vanishes at the phase transition temperature of the surface magnetization at the junction. The equations (6) and (7) show that the Josephson current flows only in the region within $\lambda_J(T)$ from the edges of the junction. Accordingly, it is expected that when temperature is lowered and $\lambda_J(T)$ decreases, the maximum Josephson current diminishes and finally vanishes at the phase transition temperature of the surface magnetization of the junction. This temperature dependence of the maximum of the Josephson current has really been observed by Umbach and Goldman using the junction of $ErRh_4B_4$-Lu_xO_y-In [57].

Figure 10 shows the magnetic field dependence of the maximum Josephson current J_{max} for the two junctions with the width of $L/\lambda_J = 0.5$ and 2. In the case of $L/\lambda_J = 0.5$, the maximum current shows the Fraunhofer patterns shown in Fig. 10(a). When temperature is lowered, the period of the Fraunhofer pattern decreases with keeping the amplitude constant. On the other hand,

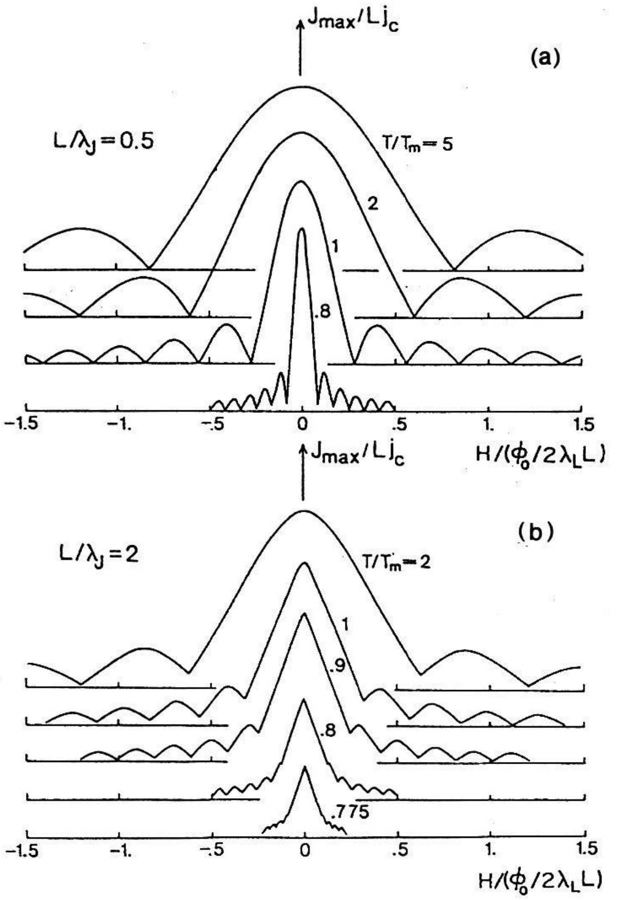

Figure 10
Field dependence of the maximum Josephson current.

in the case of $L/\lambda_J = 2$, both the amplitude and the period decreases when temperature is lowered as shown in Fig. 10(b). At low temperatures, the shape of the Fraunhofer patterns are broken down in this case.

I would like to conclude this article with adding the followings. We construct a multilayered sample in which the films of a ferromagnetic superconductor and a nonmagnetic superconductor are alternately stacked up. When the vortices are inserted into the sample by applying an external magnetic field, the vortices are more stable in the films of the ferromagnetic superconductor than in the films of the nonmagnetic superconductor. Therefore, the interfaces between the two kinds of films work as pinning centers. By using this sample it may be possible to obtain a considerably large critical current.

In rare earth compounds, the cerium compounds are special. In the compounds, the quantum mechanical mixing between the wave functions of the conduction electron and the 4f electron of Ce is strong, and in some compounds the Kondo lattice is constructed. In $CeCu_2Si_2$ the specific heat, the electrical conductivity etc. show a typical behavior of the Kondo lattice. In spite of this, the compound shows superconductivity below 0.6K [13,58]. Very recently, $CeIn_3$ was found to have similar properties. The electrical conductivity shows the Kondo lattice behavior above the antiferromagnetic transition temperature of $\sim$10K. The crystal makes a superconducting phase transition at 6 $\sim$ 7K [59]. The superconductivity in the Kondo lattice will briefly be discussed in the talk.

The author would like to express his thanks to Mr. H. Kojima, Prof. A. Kotani, Dr. T. Koyama, Dr. S. Maekawa, Prof. H. Matsumoto, Prof. O. Sakai, Mr. M. Suzuki, Mr. S. Takahashi, and Prof. H. Umezawa for valuable discussions.

REFERENCES

[1] V.L. Ginzburg, Soviet Phys. JETP *4*, 153 (1957).

[2] ϕ. Fischer, A. Treyvaud, R. Chevrel and M. Sergent, Solid State Commun. *17*, 721 (1975).

[3] B.T. Matthias, E. Corentzwit, J.M. Vandenberg and H.E. Barz, Proc. Natl. Acad. Sci. USA *74*, 1334 (1977).

[4] M. Ishikawa and ϕ. Fischer, Solid State Commun. *23*, 37 (1977); ibid *24*, 37 (1977).

[5] W.A. Fertig, D.C. Johnston, L.E. DeLong, R.W. McCallum, M.B. Maple and B.T. Matthias, Phys. Rev. Lett. *38*, 987 (1977).

[6] See, for example, M.B. Maple and ϕ. Fischer (eds.), *Superconductivity in ternary compounds II*, Topics in Current Physics, Vol. *34* (Springer-Verlag, 1982).

[7] D.C. Johnston, Solid State Commun. *24*, 699 (1977).

[8] H.C. Ku, B.T. Matthias and H. Barz, Solid State Commun. *32*, 937 (1979).

[9] K. Yvon and D.C. Johnston, Acta Cryst. *B38*, 247 (1982).

[10] J.P. Remeika, G.P. Espinosa, A.S. Cooper, H. Barz, J.M. Rowell, D.B. McWahn, J.M. Vandenberg, D.E. Moncton, Z. Fisk, L.D. Woolf, H.C. Hamaker, M.B. Maple, G. Shirane and W. Thomlinson, Solid State Commun. *34*, 923

(1980).

[11] H.F. Braun, Phys. Lett. *75 A*, 386 (1980).

[12] H.F. Braun, K. Yvon and R.M. Braun, Acta Cryst. *B36*, 2397 (1980).

[13] F. Steglich, J. Aarts, C.D. Bredl, W. Leike, D. Meschede, W. Franz and H. Schäfer, Phys. Rev. Lett. *43*, 1892 (1979).

[14] A. Kolodziejczyk, B.V.B. Sarkissian and B.R. Coles, J. Phys. *F10*, L333 (1980).

[15] K. Bechgaard, K. Carneiro, M. Olsen, F.B. Ramussen and C.S. Jacobsen, Phys. Rev. Lett. *46*, 852 (1981).

[16] D. Jérome, A. Mazaud, M. Ribault and K. Bechgaard, J. Phys. Lett. *41*, L-95 (1980).

[17] S.S.P. Parkin, M. Ribalts, D. Jérome and K. Bechgaard, J. Phys. *C14*, L445 (1981).

[18] A.A. Abrikosov and L.D. Gorkov, Soviet Phys. JETP *12*, 1243 (1961).

[19] D. Rainer, Z. Phys. *252*, 174 (1972).

[20] A. Sakurai, Solid State Commun. *25*, 867 (1978).

[21] S. Maekawa and M. Tachiki, Phys. Rev. *B18*, 4688 (1978).

[22] K. Machida and D. Youngner, J. Low Temp. Phys. *35*, 449 (1979); ibid *35*, 561 (1979).

[23] C.Y. Huang, S.E. Kohn, S. Maekawa and J.L. Smith, Solid State Commun. *32*, 929 (1979).

[24] O. Sakai, M. Suzuki, S. Maekawa and M. Tachiki, J. Phys. Soc. Jpn. *52*, No. 4 (1983).

[25] K. Machida, K. Nokura and T. Matsubara, Phys. Rev. *B22*, 2307 (1980).

[26] M.J. Nass, K. Levin and G.S. Grest, Phys. Rev. Lett. *46*, 614 (1981).

[27] Y. Suzumura and A.D.S. Nagi, Solid State Commun. *40*, 651 (1981); ibid *41*, 413 (1982).

[28] G. Zwicknagl and P. Fulde, Z. Phys. *B43*, 23 (1981).

[29] E.I. Blount and C.M. Varma, Phys. Rev. Lett. *42*, 1079 (1979).

[30] H. Matsumoto, H. Umezawa and M. Tachiki, Solid State Commun. *31*, 157 (1979).

[31] M. Tachiki, A. Kotani, H. Matsumoto and H. Umezawa, Solid State Commun. *31*, 927 (1979).

[32] R.A. Ferrell, J.K. Bhattacharjee and A. Bagchi, Phys. Rev. Lett. *43*, 154 (1979).

[33] J.W. Lynn, G. Shirane, W. Thomlinson, R.N. Shelton and D.E. Moncton,

Phys. Rev. *B24* , 3817 (1981).

[34] J.W. Lynn, J.L. Ragazzoni, R. Pynn and J. Joffrin, J. Phys. Lett. (France) *42*, L-45 (1981).

[35] D.E. Moncton, G. Shirane and W. Thomlinson, J. Magn. Magn. Mater. *14*, 172 (1979).

[36] S.K. Sinha, G.W. Crabtree, D.G. Hinks and H. Mook, Phys. Rev. Lett. *48*, 2060 (1982).

[37] M. Tachiki, A. Kotani, H. Matsumoto and H. Umezawa, Solid State Commun. *32*, 599 (1979),

[38] M. Tachiki, S. Takahashi, H. Matsumoto and H. Umezawa, Solid State Commun. *34*, 393 (1980).

[39] M. Tachiki, H. Matsumoto and H. Umezawa, Phys. Rev. *B20*, 1915 (1979).

[40] S. Maekawa, M. Tachiki and S. Takahashi, J. Magn. Magn. Mater. *13*, 324 (1979).

[41] M. Tachiki, H. Matsumoto, T. Koyama and H. Umezawa, Solid State Commun. *34*, 19 (1980).

[42] T. Koyama, S. Maekawa and M. Tachiki, J. Phys. Soc. Jpn. *52*, No.5 (1983).

[43] M. Suzuki and M. Tachiki, to be published.

[44] G.W. Crabtree, private communication.

[45] C.G. Kuper, M. Revzen and A. Ron, Phys. Rev. Lett. *44*, 1545 (1980).

[46] H.S. Greenside, E.I. Blount and C.M. Varma, Phys. Rev. Lett. *46*, 49 (1981).

[47] O. Sakai, M. Tachiki, H. Matsumoto and H. Umezawa, Solid State Commun. *39*, 279 (1981).

[48] A. Kotani, M. Tachiki, H. Matsumoto, H. Umezawa and S. Takahashi, Phys. Rev. *B23*, 5960 (1981).

[49] M. Tachiki, A. Kotani, S. Takahashi, T. Koyama, H. Matsumoto and H. Umezawa, Solid State Commun. *37*, 113 (1981).

[50] T. Koyama, A. Kotani, S. Takahashi, M. Tachiki, H. Matsumoto and H. Umezawa, J. Phys. Soc. Jpn. *51*, 3469 (1982).

[51] M. Tachiki, T. Koyama and S. Takahashi, J. Magn. Magn. Mater. *35*, to be published (1983).

[52] A. Kotani, S. Takahashi, M. Tachiki, H. Matsumoto and H. Umezawa, Solid State Commun. *37*, 619 (1981).

[53] S. Takahashi, A. Kotani, M. Tachiki, H. Matsumoto and H. Umezawa, J. Phys. Soc. Jpn. *52*, 989 (1983).

[54] S. Takahashi and M. Tachiki, to be published.

[55] B.D. Josephson, Advan. Phys. *14*, 419 (1965).

[56] S. Takahashi, T. Koyama and M. Tachiki, to be published.

[57] C.P. Umbach and A.M. Goldman, Phys. Rev. Lett. *48*, 1433 (1982).

[58] W. Leike, U. Rauchschwalbe, C.D. Bredl, F. Steglich, S. Aarts and F.R. Boer, J. Appl. Phys. *53*, 2111 (1982).

[59] M. Sera and T. Kasuya, private communication.